

# Type III interferons disrupt the lung epithelial barrier upon viral recognition

Achille Broggi<sup>1\*</sup>, Sreya Ghosh<sup>1\*</sup>, Benedetta Sposito<sup>1,2\*</sup>, Roberto Spreafico<sup>3†</sup>, Fabio Balzarini<sup>1,2</sup>, Antonino Lo Cascio<sup>1,2</sup>, Nicola Clementi<sup>4</sup>, Maria De Santis<sup>5</sup>, Nicasio Mancini<sup>4,6</sup>, Francesca Granucci<sup>2,7</sup>, Ivan Zanoni<sup>1,2,8‡</sup>

<sup>1</sup>Harvard Medical School, Boston Children's Hospital, Division of Immunology, Boston, MA, USA. <sup>2</sup>Department of Biotechnology and Biosciences, University of Milano - Bicocca, Milan, Italy. <sup>3</sup>Institute for Quantitative and Computational Biosciences, University of California, Los Angeles, CA, USA. <sup>4</sup>Laboratory of Medical Microbiology and Virology, Vita-Salute San Raffaele University, Milan, Italy. <sup>5</sup>Rheumatology and Clinical Immunology, Humanitas Clinical and Research Center - IRCCS, Rozzano, Italy. <sup>6</sup>IRCCS San Raffaele Hospital, Milan, Italy. <sup>7</sup>INGM-National Institute of Molecular Genetics "Romeo ed Enrica Invernizzi" Milan, Italy. <sup>8</sup>Harvard Medical School, Boston Children's Hospital, Division of Gastroenterology, Boston, MA, USA.

\*These authors contributed equally to this work.

†Present address: Vir Biotechnology, San Francisco, CA, USA.

‡Corresponding author. Email: [ivan.zanoni@childrens.harvard.edu](mailto:ivan.zanoni@childrens.harvard.edu)

**Lower respiratory tract viral infections are a leading cause of mortality. Mounting evidence indicates that most severe cases are characterized by aberrant immune responses and do not depend on viral burden. Here, we assessed how type III interferons (IFN- $\lambda$ ) contribute to the pathogenesis induced by RNA viruses. We report IFN- $\lambda$  is present in the lower, but not upper, airways of COVID-19 patients. In mice, we demonstrate IFN- $\lambda$  produced by lung dendritic cells in response to a synthetic viral RNA induces barrier damage, causing susceptibility to lethal bacterial superinfections. These findings provide a strong rationale for rethinking the pathophysiological role of IFN- $\lambda$  and its possible use in the clinical practice against endemic viruses, such as influenza virus, as well as the emerging SARS-CoV-2 viral infection.**

The ability to resolve viral infections of the lung is dependent on the actions of interferons (IFNs) and inflammatory cytokines, yet their relative contributions to host defense and return to homeostasis remain undefined. In particular, type III IFNs (IFN- $\lambda$ ) have attracted much attention, as they operate primarily at mucosal surfaces (1). Recent work established that, unlike other IFNs, IFN- $\lambda$  signaling induces antiviral activities while simultaneously limiting the tissue-damaging functions of neutrophils (2–4). When considered in the context of respiratory viral infections where inflammation appears to be the primary driver of life-threatening symptoms, including the recently emerged severe acute respiratory syndrome (SARS)-coronavirus (CoV)-2 (5), the ability of IFN- $\lambda$  to limit immunopathology but maintain antiviral activity is significant. Indeed, discussions on the possible use of IFN- $\lambda$  against SARS-CoV-2 have begun (6) and a clinical trial (NCT04331899) has been initiated. Despite this interest in the use of IFN- $\lambda$  to treat viral infections, the long-term effects IFN- $\lambda$  on lung physiology remain largely overlooked. For example, during viral infections of the lung, immunopathology may predispose the host to opportunistic bacterial infections and IFN- $\lambda$  impairs bacterial control during superinfections (7, 8). It remains unresolved whether this is due to the anti-inflammatory activity of IFN- $\lambda$ , which reduces host

resistance, or due to the capacity of IFN- $\lambda$  to alter lung physiology upon a viral encounter. Indeed, superinfections represent the first cause of lethality upon influenza virus infection (9) and correlate with severity in coronavirus disease (COVID)-19 patients (10).

Mouse models of SARS, middle east respiratory syndrome (MERS) (11, 12) and influenza (1, 13) are characterized by a robust induction of type I and III IFNs. However, the involvement of these cytokines in COVID-19 is controversial (14, 15). To directly evaluate the capacity of SARS-CoV-2 to induce IFNs, we tested naso-oropharyngeal swabs of COVID-19 patients and healthy controls, as well as the bronchoalveolar lavage fluid (BALF) of severe SARS-CoV-2-positive patients. Levels of IFN mRNAs in the upper airways of COVID-19 patients were not significantly different from healthy controls. By contrast, BALF of patients with severe disease presented elevated levels of both inflammatory cytokines as well as type I and III IFNs (Fig. 1, A to E).

To evaluate the contribution of IFN- $\lambda$  to the immunopathology driven by RNA respiratory viruses uncoupled from its effect on viral replication, we devised an experimental system in which pattern recognition receptors (PRRs) involved in viral sensing were stimulated with their cognate ligands. RNA viruses are sensed via either endosomal toll-like receptor (TLR)-3 and TLR-7 or cytoplasmic retinoic acid-inducible

gene I (RIG-I) and melanoma differentiation-associated protein 5 (MDA5) (16). We intratracheally instilled the TLR7 ligand, R848, or the synthetic analog of double-stranded RNA, polyinosine:polycytidylic acid (poly (I:C)), that stimulates both TLR3 and the RIG-I-MDA5 pathway in vivo (17). PRRs were stimulated over the course of 6 days to elicit prolonged innate immune activation in the lung. Both ligands induced hypothermia (Fig. 1F) and weight loss (fig. S1A), but only poly (I:C) compromised barrier function (Fig. 1G and fig. S1B). IFN mRNAs were strongly up-regulated by poly (I:C) but not R848 (Fig. 1, H and I). By contrast, R848 treatment induced the up-regulation of pro-inflammatory cytokines (i.e., *Il1b*) but this did not correlate with barrier function decrease (Fig. 1, G to J, and fig. S1B).

Alterations in the epithelial barrier predispose to lethal bacterial superinfections (18). We therefore infected mice treated with either R848 or poly (I:C) with *Staphylococcus aureus*. Mice treated with poly (I:C) died upon *S. aureus* infection (Fig. 1K) and had higher bacterial burdens (Fig. 1L), more intense hypothermia, and greater barrier damage (fig. S2, A and B). *S. aureus* infection did not alter the pattern of cytokine expression (fig. S2, C to E). Upon poly (I:C) administration, IFN- $\beta$  and IFN- $\lambda$  transcript and protein levels were rapidly up-regulated and plateaued (fig. S3, A to D), while *S. aureus* bacterial burden increased over time (fig. S3E). IFN-stimulated genes (ISGs), but not pro-inflammatory cytokines, were also sustained over time (fig. S3, F to I). These data suggest that chronic exposure to IFNs aggravates bacterial superinfections. Since the protein levels of IFN- $\lambda$  were very high compared to IFN- $\beta$  (fig. S3, C and D), we assessed if IFN- $\lambda$  was sufficient to exacerbate bacterial superinfections. We administered exogenous IFN- $\lambda$  either alone, or with R848, which induces inflammation but not IFN production (Fig. 1, H to J). The administration of IFN- $\lambda$  with R848, but not IFN- $\lambda$  alone, was sufficient to induce sensitivity to *S. aureus* infection (Fig. 1, M and N, and fig. S3J). Thus, in an inflamed lung, IFN- $\lambda$  is sufficient to aggravate superinfections.

In contrast to wild-type (WT) mice, mice deficient in IFN- $\lambda$  receptor 1 (*Ifnlr1*) expression were protected from poly (I:C)-induced morbidity and barrier damage (Fig. 2, A and B, and fig. S4, A and B). *Ifnlr1*<sup>-/-</sup> mice superinfected with *S. aureus* were also protected (Fig. 2C-F) compared to WT mice. By contrast, the absence of *Ifnlr1* did not impact mRNA or protein levels of IFNs or pro-inflammatory cytokines (fig. S4, C to H). We next generated reciprocal bone marrow chimeras in which either the hematopoietic or the stromal compartments were defective for IFN- $\lambda$  signaling. Absence of *Ifnlr1* in the stromal compartment, but not in hematopoietic cells, phenocopied complete *Ifnlr1* deficiency (Fig. 2, G and H, and fig. S5). Furthermore, there was no difference in myeloid immune cell recruitment in *Ifnlr1*<sup>-/-</sup> compared to WT mice (fig. S6, A to D) and depletion of neutrophils did not impact

bacterial burden (fig. S6E). Thus, IFN- $\lambda$  signaling in epithelial cells is necessary and sufficient to induce susceptibility to a secondary infection.

A targeted transcriptomic analysis on lung epithelial cells from mice treated with poly (I:C) revealed a potent down-regulation of the IFN signature in *Ifnlr1*<sup>-/-</sup> compared to WT mice (Fig. 3, A and B, fig. S7, and data S1). This confirmed the predominant role of IFN- $\lambda$  compared to type I IFNs during prolonged viral sensing in the lung. Consistent with the observed defect in barrier function, genes associated with apoptosis and the activation of the p53 pathway were enriched in WT compared to *Ifnlr1*<sup>-/-</sup> epithelial cells (Fig. 3B). By contrast, pathways involved in positive regulation of the cell cycle were enriched in *Ifnlr1*<sup>-/-</sup> cells (Fig. 3C). Accordingly, epithelial cells in *Ifnlr1*<sup>-/-</sup> mice, as well as in stromal *Ifnlr1*<sup>-/-</sup> chimeras, proliferated more efficiently after poly (I:C) administration, in the presence or absence of *S. aureus* (Fig. 3, D to G). The most down-regulated gene in *Ifnlr1*<sup>-/-</sup> epithelial cells compared to WT cells was the E3 ubiquitin-protein ligase markerin-1 (*Mkrn1*) (Fig. 3A and data S1). This protein induces p21 degradation and favors apoptosis via p53 under oxidative stress conditions and after DNA damage (hallmarks of severe viral infections) (19). Indeed, *Ifnlr1*<sup>-/-</sup> epithelial cells showed elevated levels of p21 (Fig. 3, H and I). Thus, the ability of IFN- $\lambda$  to reduce tissue tolerance stems from its capacity to inhibit tissue repair by directly influencing epithelial cell proliferation and viability.

We next investigated the cellular source and molecular pathways that drive IFN- $\lambda$  production. Upon poly (I:C) administration, lung-resident dendritic cells (DCs) expressed the highest levels of IFN- $\lambda$  transcript, both during the early and late phases following poly (I:C) administration (Fig. 4A and fig. S8A). By contrast, epithelial cells, alveolar macrophages, and monocytes expressed type I IFNs and pro-inflammatory cytokines but no IFN- $\lambda$  transcripts (fig. S8, A to C). Depletion of CD11c<sup>+</sup> DCs was sufficient to abolish the production of IFN- $\lambda$  but not type I IFNs (Fig. 4, B and C, and fig. S8, D and E). Alveolar macrophages were not depleted under our experimental conditions (fig. S8F) and did not produce IFN- $\lambda$  (Fig. 4A). By using in vitro-generated DCs, we found that IFN- $\lambda$  was induced only when the TLR3 pathway was activated (Fig. 4D and fig. S9, A and B). Consistent with in vivo data, TLR7 stimulation in vitro induced only the up-regulation of pro-inflammatory cytokines (Fig. 4D and fig. S9, A and B). Ex vivo analysis showed that conventional (c)DC1 are the major producer of IFN- $\lambda$  (fig. S10). Activation of RIG-I/MDA5 via intracellular delivery of poly (I:C) (Fig. 4D and fig. S9, A and B) and of 3-phosphate-hairpin-RNA (3p-hpRNA, fig. S11, A to E) induced high levels of type I IFNs, but not type III IFNs in a mitochondrial antiviral signaling protein (MAVS)-dependent manner. Blockade of endosomal acidification via chloroquine treatment confirmed the importance of TLR3 for

IFN- $\lambda$  induction (fig. S12, A and B). WT mice or mice that do not respond to TLR3 stimulation (Toll-like receptor adaptor molecule 1 deficient (*Ticam1*<sup>-/-</sup>)) were treated in vivo with poly (I:C). Only DCs sorted from *Ticam1*<sup>-/-</sup> mice did not express IFN- $\lambda$  mRNA although they still expressed type I IFN mRNA, Fig. 4, E and F). Furthermore, *Ticam1*<sup>-/-</sup> mice were protected against *S. aureus* superinfections (Fig. 4G). *Ticam1*<sup>-/-</sup> mice also showed lower IFN- $\lambda$  (but not type I IFN) mRNA levels (Fig. 4, H and I). Similar results were obtained when only hematopoietic cells were deficient in *Ticam1* (Fig. 4, J to L).

The immune system evolved to protect against pathogens but doing so often threatens host fitness and can cause immunopathologies (20). In COVID-19, SARS, MERS, and flu, severe symptoms and death occur late, and after the peak in viral load, indicating a central role for the immune system in driving the pathology (21–24). In our system, we isolated the effect of immune activation from resistance to lung viral infections and demonstrated that sustained IFN- $\lambda$  is produced by DCs via TLR3. TLR3 detects replication intermediates from dying cells (25) and is, thus, insensitive to viral immune evasion. Thus, IFN- $\lambda$  acts on lung epithelial cells and compromises lung barrier function predisposing the host to lethal secondary bacterial infections.

Previous findings suggested that IFN- $\lambda$  protects against viral infections (26) and increases the barrier functions of gut epithelial cells as well as of endothelial cells (27–29). These discrepancies can be explained by the fact that the particular cell types targeted by IFN- $\lambda$  in those studies were different. Furthermore, our data support the hypothesis that the detrimental activities of IFN- $\lambda$  only occur upon chronic exposure and in the presence of tissue damage. Indeed, the early administration of IFN- $\lambda$  in a mouse model of COVID-19 could confer protection (30). In conclusion, our data enjoin clinicians to carefully analyze the duration of IFN- $\lambda$  administration and to take into consideration the severity of disease when IFN- $\lambda$  is used as a therapeutic agent against lung viral infections.

## REFERENCES AND NOTES

1. A. Broggi, F. Granucci, I. Zanoni, Type III interferons: Balancing tissue tolerance and resistance to pathogen invasion. *J. Exp. Med.* **217**, e20190295 (2020). [doi:10.1084/jem.20190295](https://doi.org/10.1084/jem.20190295) [Medline](#)
2. A. Broggi, Y. Tan, F. Granucci, I. Zanoni, IFN- $\lambda$  suppresses intestinal inflammation by non-translational regulation of neutrophil function. *Nat. Immunol.* **18**, 1084–1093 (2017). [doi:10.1038/ni.3821](https://doi.org/10.1038/ni.3821) [Medline](#)
3. I. E. Galani, V. Triantafyllia, E.-E. Eleminiadou, O. Koltsida, A. Stavropoulos, M. Manioudaki, D. Thanos, S. E. Doyle, S. V. Kolenko, K. Thanopoulou, E. Andreacos, Interferon- $\lambda$  Mediates Non-redundant Front-Line Antiviral Protection against Influenza Virus Infection without Compromising Host Fitness. *Immunity* **46**, 875–890.e6 (2017). [doi:10.1016/j.immuni.2017.04.025](https://doi.org/10.1016/j.immuni.2017.04.025) [Medline](#)
4. K. Blazek, H. L. Eames, M. Weiss, A. J. Byrne, D. Perocheau, J. E. Pease, S. Doyle, F. McCann, R. O. Williams, I. A. Udalova, IFN- $\lambda$  resolves inflammation via suppression of neutrophil infiltration and IL-1 $\beta$  production. *J. Exp. Med.* **212**, 845–853 (2015). [doi:10.1084/jem.20140995](https://doi.org/10.1084/jem.20140995) [Medline](#)
5. M. Merad, J. C. Martin, Pathological inflammation in patients with COVID-19: A key role for monocytes and macrophages. *Nat. Rev. Immunol.* **20**, 355–362 (2020). [doi:10.1038/s41577-020-0331-4](https://doi.org/10.1038/s41577-020-0331-4) [Medline](#)
6. L. Prokunina-Olsson, N. Alphonse, R. E. Dickenson, J. E. Durbin, J. S. Glenn, R. Hartmann, S. V. Kolenko, H. M. Lazear, T. R. O'Brien, C. Odendall, O. O. Onabajo, H. Piontkivska, D. M. Santer, N. C. Reich, A. Wack, I. Zanoni, COVID-19 and emerging viral infections: The case for interferon lambda. *J. Exp. Med.* **217**, e20200653 (2020). [doi:10.1084/jem.20200653](https://doi.org/10.1084/jem.20200653) [Medline](#)
7. H. E. Rich, C. C. McCourt, W. Q. Zheng, K. J. McHugh, K. M. Robinson, J. Wang, J. F. Alcorn, Interferon Lambda Inhibits Bacterial Uptake during Influenza Superinfection. *Infect. Immun.* **87**, e00114-19 (2019). [doi:10.1128/IAI.00114-19](https://doi.org/10.1128/IAI.00114-19) [Medline](#)
8. P. J. Planet, D. Parker, T. S. Cohen, H. Smith, J. D. Leon, C. Ryan, T. J. Hammer, N. Fierer, E. I. Chen, A. S. Prince, Lambda Interferon Restructures the Nasal Microbiome and Increases Susceptibility to *Staphylococcus aureus* Superinfection. *mBio* **7**, e01939-15 (2016). [doi:10.1128/mBio.01939-15](https://doi.org/10.1128/mBio.01939-15) [Medline](#)
9. J. A. McCullers, The co-pathogenesis of influenza viruses with bacteria in the lung. *Nat. Rev. Microbiol.* **12**, 252–262 (2014). [doi:10.1038/nrmicro3231](https://doi.org/10.1038/nrmicro3231) [Medline](#)
10. G. Zhang, C. Hu, L. Luo, F. Fang, Y. Chen, J. Li, Z. Peng, H. Pan, Clinical features and short-term outcomes of 221 patients with COVID-19 in Wuhan, China. *J. Clin. Virol.* **127**, 104364 (2020). [doi:10.1016/j.jcv.2020.104364](https://doi.org/10.1016/j.jcv.2020.104364) [Medline](#)
11. R. Channappanavar, A. R. Fehr, J. Zheng, C. Wohlford-Lenane, J. E. Abrahante, M. Mack, R. Sompallae, P. B. McCray Jr., D. K. Meyerholz, S. Perlman, IFN-I response timing relative to virus replication determines MERS coronavirus infection outcomes. *J. Clin. Invest.* **129**, 3625–3639 (2019). [doi:10.1172/JCI126363](https://doi.org/10.1172/JCI126363) [Medline](#)
12. M. B. Frieman, J. Chen, T. E. Morrison, A. Whitmore, W. Funkhouser, J. M. Ward, E. W. Lamirande, A. Roberts, M. Heise, K. Subbarao, R. S. Baric, SARS-CoV pathogenesis is regulated by a STAT1 dependent but a type I, II and III interferon receptor independent mechanism. *PLOS Pathog.* **6**, e1000849 (2010). [doi:10.1371/journal.ppat.1000849](https://doi.org/10.1371/journal.ppat.1000849) [Medline](#)
13. J. Major, S. Crotta, M. Llorian, T. M. McCabe, H. H. Gad, S. L. Priestnall, R. Hartmann, A. Wack, Type I and III interferons disrupt lung epithelial repair during recovery from viral infection. *Science* **10.1126/science.abc2061** (2020). [doi:10.1126/science.abc2061](https://doi.org/10.1126/science.abc2061)
14. D. Blanco-Melo, B. E. Nilsson-Payant, W.-C. Liu, S. Uhl, D. Hoagland, R. Møller, T. X. Jordan, K. Oishi, M. Panis, D. Sachs, T. T. Wang, R. E. Schwartz, J. K. Lim, R. A. Albrecht, B. R. tenOever, Imbalanced Host Response to SARS-CoV-2 Drives Development of COVID-19. *Cell* **181**, 1036–1045.e9 (2020). [doi:10.1016/j.cell.2020.04.026](https://doi.org/10.1016/j.cell.2020.04.026) [Medline](#)
15. Z. Zhou, L. Ren, L. Zhang, J. Zhong, Y. Xiao, Z. Jia, L. Guo, J. Yang, C. Wang, S. Jiang, D. Yang, G. Zhang, H. Li, F. Chen, Y. Xu, M. Chen, Z. Gao, J. Yang, J. Dong, B. Liu, X. Zhang, W. Wang, K. He, Q. Jin, M. Li, J. Wang, Heightened Innate Immune Responses in the Respiratory Tract of COVID-19 Patients. *Cell Host Microbe* **27**, 883–890.e2 (2020). [doi:10.1016/j.chom.2020.04.017](https://doi.org/10.1016/j.chom.2020.04.017) [Medline](#)
16. A. Iwasaki, P. S. Pillai, Innate immunity to influenza virus infection. *Nat. Rev. Immunol.* **14**, 315–328 (2014). [doi:10.1038/nri3665](https://doi.org/10.1038/nri3665) [Medline](#)
17. H. Kato, O. Takeuchi, S. Sato, M. Yoneyama, M. Yamamoto, K. Matsui, S. Uematsu, A. Jung, T. Kawai, K. J. Ishii, O. Yamaguchi, K. Otsu, T. Tsujimura, C.-S. Koh, C. Reis e Sousa, Y. Matsuura, T. Fujita, S. Akira, Differential roles of MDA5 and RIG-I helicases in the recognition of RNA viruses. *Nature* **441**, 101–105 (2006). [doi:10.1038/nature04734](https://doi.org/10.1038/nature04734) [Medline](#)
18. A. M. Jamieson, L. Pasman, S. Yu, P. Gamradt, R. J. Homer, T. Decker, R. Medzhitov, Role of tissue protection in lethal respiratory viral-bacterial coinfection. *Science* **340**, 1230–1234 (2013). [doi:10.1126/science.1233632](https://doi.org/10.1126/science.1233632) [Medline](#)
19. E. W. Lee, M.-S. Lee, S. Camus, J. Ghim, M.-R. Yang, W. Oh, N.-C. Ha, D. P. Lane, J. Song, Differential regulation of p53 and p21 by MKRN1 E3 ligase controls cell cycle arrest and apoptosis. *EMBO J.* **28**, 2100–2113 (2009). [doi:10.1038/emboj.2009.164](https://doi.org/10.1038/emboj.2009.164) [Medline](#)
20. R. Medzhitov, D. S. Schneider, M. P. Soares, Disease tolerance as a defense strategy. *Science* **335**, 936–941 (2012). [doi:10.1126/science.1214935](https://doi.org/10.1126/science.1214935) [Medline](#)
21. J. S. Peiris, C. M. Chu, V. C. C. Cheng, K. S. Chan, I. F. N. Hung, L. L. M. Poon, K. I. Law, B. S. F. Tang, T. Y. W. Hon, C. S. Chan, K. H. Chan, J. S. C. Ng, B. J. Zheng, W. L. Ng, R. W. M. Lai, Y. Guan, K. Y. Yuen; HKU/UCH SARS Study Group, Clinical progression and viral load in a community outbreak of coronavirus-associated

- SARS pneumonia: A prospective study. *Lancet* **361**, 1767–1772 (2003). [doi:10.1016/S0140-6736\(03\)13412-5](https://doi.org/10.1016/S0140-6736(03)13412-5) [Medline](#)
22. Z. A. Memish, S. Perlman, M. D. Van Kerkhove, A. Zumla, Middle East respiratory syndrome. *Lancet* **395**, 1063–1077 (2020). [doi:10.1016/S0140-6736\(19\)33221-0](https://doi.org/10.1016/S0140-6736(19)33221-0) [Medline](#)
  23. R. Wölfel, V. M. Corman, W. Guggemos, M. Seilmaier, S. Zange, M. A. Müller, D. Niemeyer, T. C. Jones, P. Vollmar, C. Rothe, M. Hoelscher, T. Bleicker, S. Brünink, J. Schneider, R. Ehmann, K. Zwirgmaier, C. Drosten, C. Wendtner, Virological assessment of hospitalized patients with COVID-2019. *Nature* **581**, 465–469 (2020). [doi:10.1038/s41586-020-2196-x](https://doi.org/10.1038/s41586-020-2196-x) [Medline](#)
  24. C. K. Lee, H. K. Lee, T. P. Loh, F. Y. L. Lai, P. A. Tambyah, L. Chiu, E. S. C. Koay, J. W. Tang, Comparison of pandemic (H1N1) 2009 and seasonal influenza viral loads, Singapore. *Emerg. Infect. Dis.* **17**, 287–291 (2011). [doi:10.3201/eid1702.100282](https://doi.org/10.3201/eid1702.100282) [Medline](#)
  25. O. Schulz, S. S. Diebold, M. Chen, T. I. Näslund, M. A. Nolte, L. Alexopoulou, Y.-T. Azuma, R. A. Flavell, P. Liljestrom, C. Reis e Sousa, Toll-like receptor 3 promotes cross-priming to virus-infected cells. *Nature* **433**, 887–892 (2005). [doi:10.1038/nature03326](https://doi.org/10.1038/nature03326) [Medline](#)
  26. L. Ye, D. Schnepf, P. Staeheli, Interferon- $\lambda$  orchestrates innate and adaptive mucosal immune responses. *Nat. Rev. Immunol.* **19**, 614–625 (2019). [doi:10.1038/s41577-019-0182-z](https://doi.org/10.1038/s41577-019-0182-z) [Medline](#)
  27. C. Odendall, A. A. Voak, J. C. Kagan, Type III IFNs Are Commonly Induced by Bacteria-Sensing TLRs and Reinforce Epithelial Barriers during Infection. *J. Immunol.* **199**, 3270–3279 (2017). [doi:10.4049/jimmunol.1700250](https://doi.org/10.4049/jimmunol.1700250) [Medline](#)
  28. H. M. Lazear, B. P. Daniels, A. K. Pinto, A. C. Huang, S. C. Vick, S. E. Doyle, M. Gale Jr., R. S. Klein, M. S. Diamond, Interferon- $\lambda$  restricts West Nile virus neuroinvasion by tightening the blood-brain barrier. *Sci. Transl. Med.* **7**, 284ra59 (2015). [doi:10.1126/scitranslmed.aaa4304](https://doi.org/10.1126/scitranslmed.aaa4304) [Medline](#)
  29. F. Douam, Y. E. Soto Albrecht, G. Hrebikova, E. Sadimin, C. Davidson, S. V. Kotenko, A. Ploss, Type III Interferon-Mediated Signaling Is Critical for Controlling Live Attenuated Yellow Fever Virus Infection In Vivo. *mBio* **8**, e00819-17 (2017). [doi:10.1128/mBio.00819-17](https://doi.org/10.1128/mBio.00819-17) [Medline](#)
  30. K. H. Dinnon III, S. R. Leist, A. Schäfer, C. E. Edwards, D. R. Martinez, S. A. Montgomery, A. West, B. L. Yount Jr., Y. J. Hou, L. E. Adams, K. L. Gully, A. J. Brown, E. Huang, M. D. Bryant, I. C. Choong, J. S. Glenn, L. E. Gralinski, T. P. Sheahan, R. S. Baric, A mouse-adapted SARS-CoV-2 model for the evaluation of COVID-19 medical countermeasures. *bioRxiv* 2020.05.06.081497 [Preprint] (2020); <https://doi.org/10.1101/2020.05.06.081497>.

## ACKNOWLEDGMENTS

We thank Dr. J.C. Kagan for discussion, help and support. **Funding:** I.Z. is supported by NIH grant 1R01AI121066, 1R01DK115217, and NIAID-DAIT-NIHAI201700100. A.B. is supported by CFA RFA 549868. F.G. is supported by AIRC (IG 2019Id.23512), Fondazione regionale per la ricerca biomedica, FRRB (IANG-CRC - CP2\_12/2018), and Ministero della Salute, Ricerca Finalizzata (RF-2018-12367072). **Author contributions:** A.B., S.G., and B.S. designed, performed, and analyzed the experiments; A.B. wrote the paper; R.S. performed the analysis of the sequencing data; F.B. and A.L.C. performed the experiments; N.C., M.D.S., and N.M. performed and analyzed human experiments; F.G. contributed to the design of the experiments; I.Z. conceived the project, designed the experiments, supervised the study and wrote the paper. **Competing interests:** The authors declare no commercial or financial conflict of interest. **Data and materials availability:** All data are available in the manuscript or the supplementary materials. Use of *Irfn1*<sup>-/-</sup> mice and polyethylene glycol-conjugated IFN- $\lambda$ 2 was performed under a MTA with Bristol-Myers Squibb. This work is licensed under a Creative Commons Attribution 4.0 International (CC BY 4.0) license, which permits unrestricted use, distribution, and reproduction in any medium, provided the original work is properly cited. To view a copy of this license, visit <https://creativecommons.org/licenses/by/4.0/>. This license does not apply to figures/photos/artwork or other content included in the article that is credited to a third party; obtain authorization from the rights holder before using such material.

## SUPPLEMENTARY MATERIALS

[science.sciencemag.org/cgi/content/full/science.abc3545/DC1](https://science.sciencemag.org/cgi/content/full/science.abc3545/DC1)

Materials and Methods

Figs. S1 to S13

Tables S1 to S3

MDAR Reproducibility Checklist

Data S1

21 April 2020; accepted 8 June 2020

Published online 11 June 2020

10.1126/science.abc3545

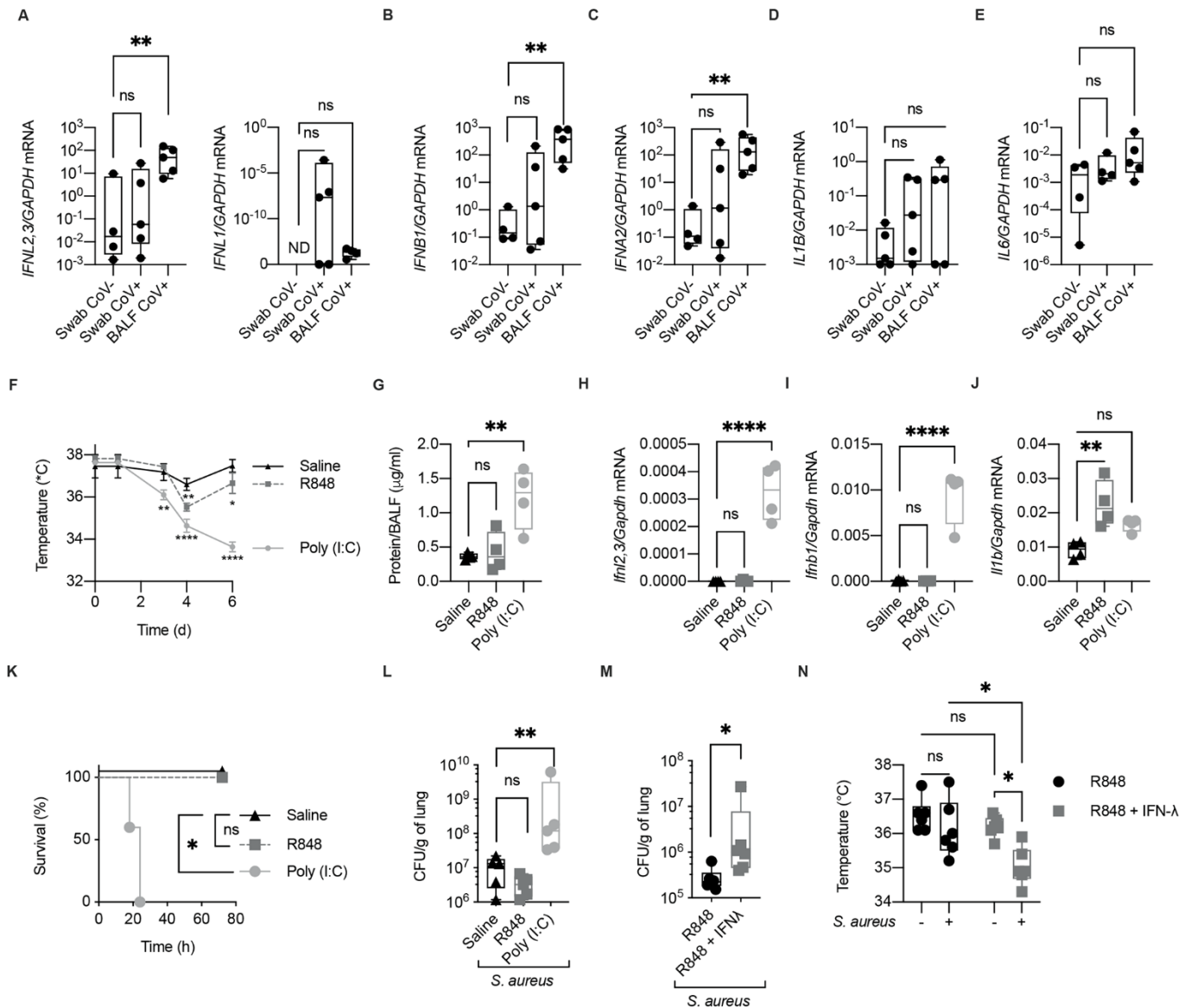


**Fig. 1. Morbidity correlates with the high expression of type I IFN and IFN- $\lambda$  in the lung of COVID-19 patient BALF and of poly (I:C)-treated mice.** (A to E) *IFNL2,3*, *IFNL1* (A), *IFNB* (B), *IFNA2* (C), *IL1B* (D), and *IL6* (E) mRNA expression was evaluated in naso-oro-pharyngeal swabs from SARS-CoV-2-positive (Swab CoV<sup>+</sup>) and -negative (Swab CoV<sup>-</sup>) subjects and from the BALF of intensive care unit (ICU)-hospitalized SARS-CoV-2-positive patients (BALF CoV<sup>+</sup>) (Five subjects per group). (F to J) Mice were intratracheally (i.t.) administered 2.5 mg/kg poly (I:C), 2.5 mg/kg R848, or saline daily for 6 days. (F) Body temperatures of the treated mice measured over time are represented. (G) Amount of total protein in the BALF was measured at day 6 post treatment. (H to J) *Ifnl2,3* (H), *Ifnb1* (I), and *Il1b* (J) mRNA expression were assessed in total lung lysate harvested 6 days post treatment. (K and L) Mice treated as in (F) to (J) were infected at day 6 with  $5 \times 10^7$  CFU of *S. aureus* administered i.t. and were monitored for survival (K). Bacterial loads in the lungs of the treated mice normalized to lung weight were assessed 12 hours post infection (hpi) (L). Mice were i.t. administered R848 (2.5 mg/kg) or a combination of R848 and IFN- $\lambda$  (50  $\mu$ g/kg) daily for 6 days and were then infected as in (K). Lung bacterial burdens (M) and body temperatures (N) before and after *S. aureus* infection are shown [(G) to (J), (L) to (N)]. Each symbol represents one mouse. The median and range are represented. (F) Mean  $\pm$  SD of five mice per group is represented. (G to J) Four, (L and M) five, and (N) six mice per group are represented and median and range are shown. (K) Survival plot of five mice per group. (F-N) Representative data of three independent experiments. Statistics: ns, not significant ( $P > 0.05$ ); \* $P < 0.05$ , \*\* $P < 0.01$ , \*\*\* $P < 0.001$ , and \*\*\*\* $P < 0.0001$ . Two-way ANOVA [(F) and (N)], one-way ANOVA [(G) to (J), (L)], or two-tailed  $t$  test (M) were performed. Logarithmic values were fitted when evaluating bacterial load [(L) and (M)]. Log-rank (Mantel-Cox) test, corrected for multiple comparisons was performed to evaluate survival (K).

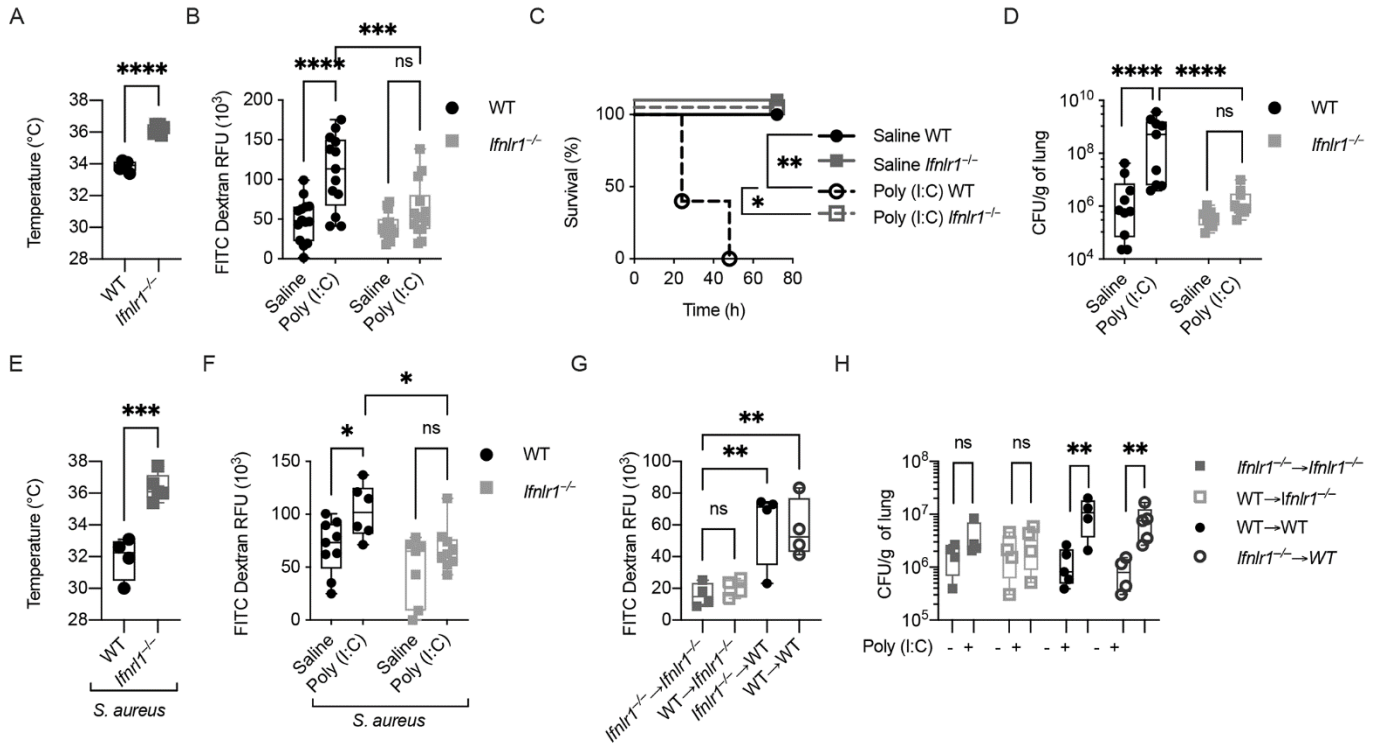


**Fig. 2. IFN- $\lambda$  is necessary to increase susceptibility to bacterial infection induced by antiviral immunity.** (A and B) WT and *Ifnlr1*<sup>-/-</sup> mice were i.t. treated with 2.5 mg/kg poly (I:C) or saline daily for 6 days. (A) Body temperatures of poly (I:C)-treated WT and *Ifnlr1*<sup>-/-</sup> mice were recorded on day 6. (B) On day 6, mice were i.t. treated with FITC-dextran (10  $\mu$ g/mouse). Barrier permeability was measured as relative fluorescent units (RFU) of FITC-dextran leaked in plasma 1 hour after injection. (C to F) WT and *Ifnlr1*<sup>-/-</sup> mice i.t. treated with 2.5 mg/kg poly (I:C) or saline for 6 days, were i.t. infected with  $5 \times 10^7$  CFU of *S. aureus* and monitored for survival (C). Lung bacterial burdens normalized by lung weight (D), body temperature (E), and barrier permeability (F) (as in (B)) were assessed 12 hpi. (G and H) Lethally irradiated WT or *Ifnlr1*<sup>-/-</sup> recipients were reconstituted with donor bone marrow (*Ifnlr1*<sup>-/-</sup> or WT) for 6 weeks and were then treated as in (C) to (F). Resulting chimeric mice were defective for IFN- $\lambda$  signaling either in the hematopoietic compartment (*Ifnlr1*<sup>-/-</sup>  $\rightarrow$  WT) or in the stromal compartment (WT  $\rightarrow$  *Ifnlr1*<sup>-/-</sup>). *Ifnlr1*<sup>-/-</sup>  $\rightarrow$  *Ifnlr1*<sup>-/-</sup>, and WT  $\rightarrow$  WT chimeras were used as controls. (G) Barrier permeability (as in (B)) and (H) lung bacterial burdens were evaluated 12 hpi. Each symbol represents one mouse. The median and range are represented. (C) Survival plot of five mice per group. (A to H) Representative data of three independent experiments. (A, E, G, and H) Four, (B) fourteen, and (D and F) ten mice per group, median and range are represented. Statistics: ns, not significant ( $P > 0.05$ ); \* $P < 0.05$ , \*\* $P < 0.01$ , \*\*\* $P < 0.001$ , and \*\*\*\* $P < 0.0001$ . Two-way ANOVA [(B), (D), (F), (H)], one-way ANOVA (G), or two-tailed  $t$  test [(A) and (E)] were performed. Logarithmic values were fitted when evaluating bacterial load [(D) and (H)]. Log-rank (Mantel-Cox) test, corrected for multiple comparisons was performed to evaluate survival (C).

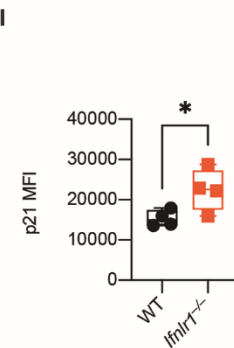
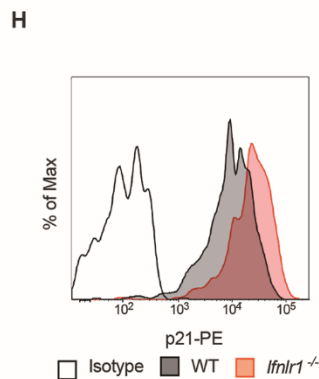
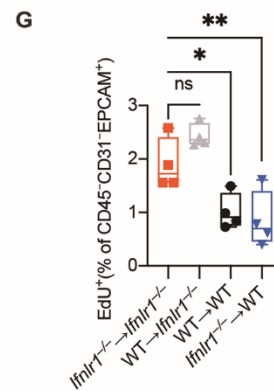
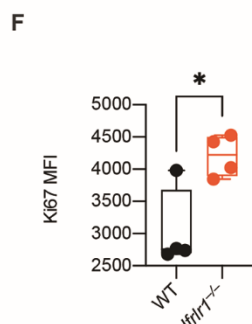
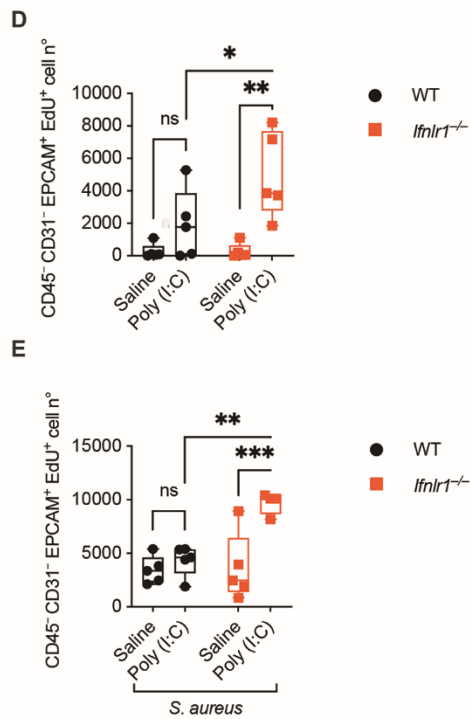
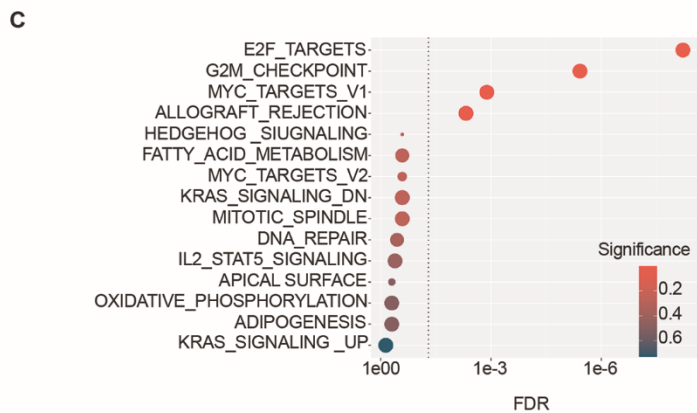
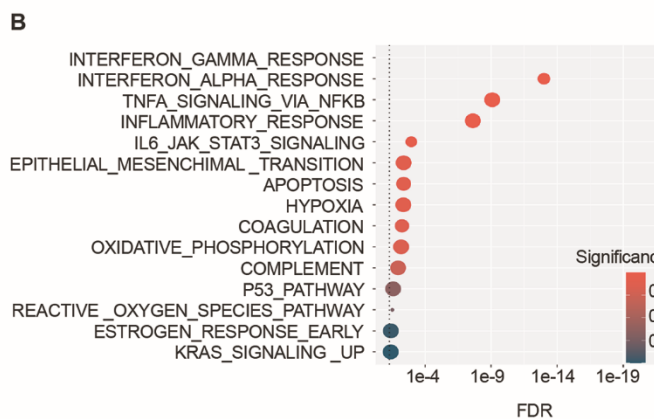
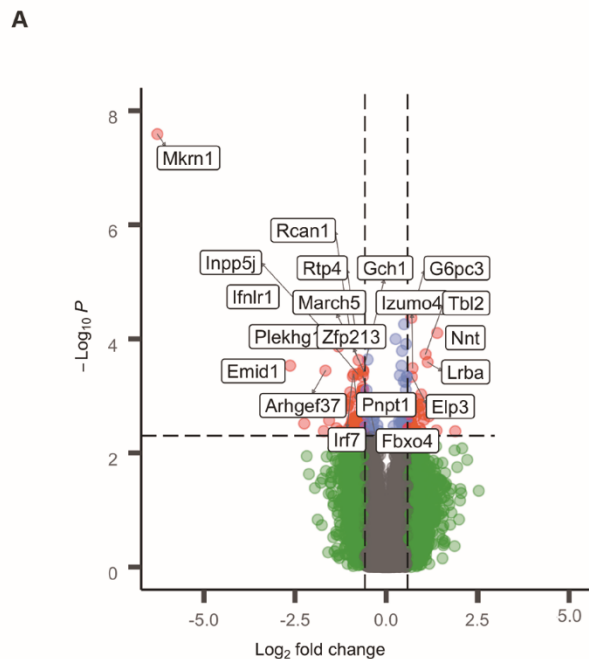


**Fig. 3. IFN- $\lambda$  signaling directly inhibits lung epithelia proliferation and impairs repair upon viral recognition.**

(A to C) Targeted transcriptome sequencing was performed on lung epithelial cells isolated on day 6 from WT and *Ifnlr1*<sup>-/-</sup> mice i.t. treated with 2.5 mg/kg poly (I:C) daily for 6 days. (A) Volcano plot of differentially expressed genes (DEGs) between WT and *Ifnlr1*<sup>-/-</sup>. DEGs ( $P < 0.005$ ) with a fold change  $>1.5$  (or  $<-1.5$ ) are indicated in red. Non-significant DEGs ( $P > 0.005$ ) are indicated in green. (B and C) Dot plot visualization of gene set enrichment analysis (GSEA) for pathways enriched in (B) WT epithelial cells compared to *Ifnlr1*<sup>-/-</sup> and (C) *Ifnlr1*<sup>-/-</sup> epithelial cells compared to WT. The color of the dots represents the adjusted  $P$ -value (significance) for each enriched pathway and its size represents the percentage of genes enriched in the total gene set. (D and E) Epithelial cell proliferation was assessed as 5-ethynyl-2'-deoxyuridine (EdU) incorporation in lung epithelial cells (CD45<sup>-</sup>CD31<sup>-</sup>EPCAM<sup>+</sup>) in WT and *Ifnlr1*<sup>-/-</sup> mice treated as in (A to C) (D), or treated as in (A to C) and i.t. infected on day 6 with  $5 \times 10^7$  CFU *S. aureus* for 12 hours (E). (F) Mean fluorescent intensity (MFI) of Ki67 in CD45<sup>-</sup>CD31<sup>-</sup>EPCAM<sup>+</sup> cells of WT and *Ifnlr1*<sup>-/-</sup> mice treated as in (A) to (C). (G) EdU incorporation in lung epithelial cells of WT or *Ifnlr1*<sup>-/-</sup> chimeric mice reconstituted with *Ifnlr1*<sup>-/-</sup> or WT bone marrow treated as in (E). (H and I) p21 levels in lung epithelial cells (CD45<sup>-</sup>CD31<sup>-</sup>EPCAM<sup>+</sup>) from WT and *Ifnlr1*<sup>-/-</sup> mice treated as in (A) to (C). Representative histogram (H) and MFI (I) are depicted. (A to C) Four mice per genotype. (D and E) Five, and (F to I) four mice per group, median and range are represented. (D to I) Representative data of three independent experiments. Statistics: ns, not significant ( $P > 0.05$ ); \* $P < 0.05$ , \*\* $P < 0.01$ , \*\*\* $P < 0.001$ , and \*\*\*\* $P < 0.0001$ . (D and E) Two-way ANOVA, (G) one-way ANOVA, (F and I), and two-tailed  $t$  test (I) were performed.



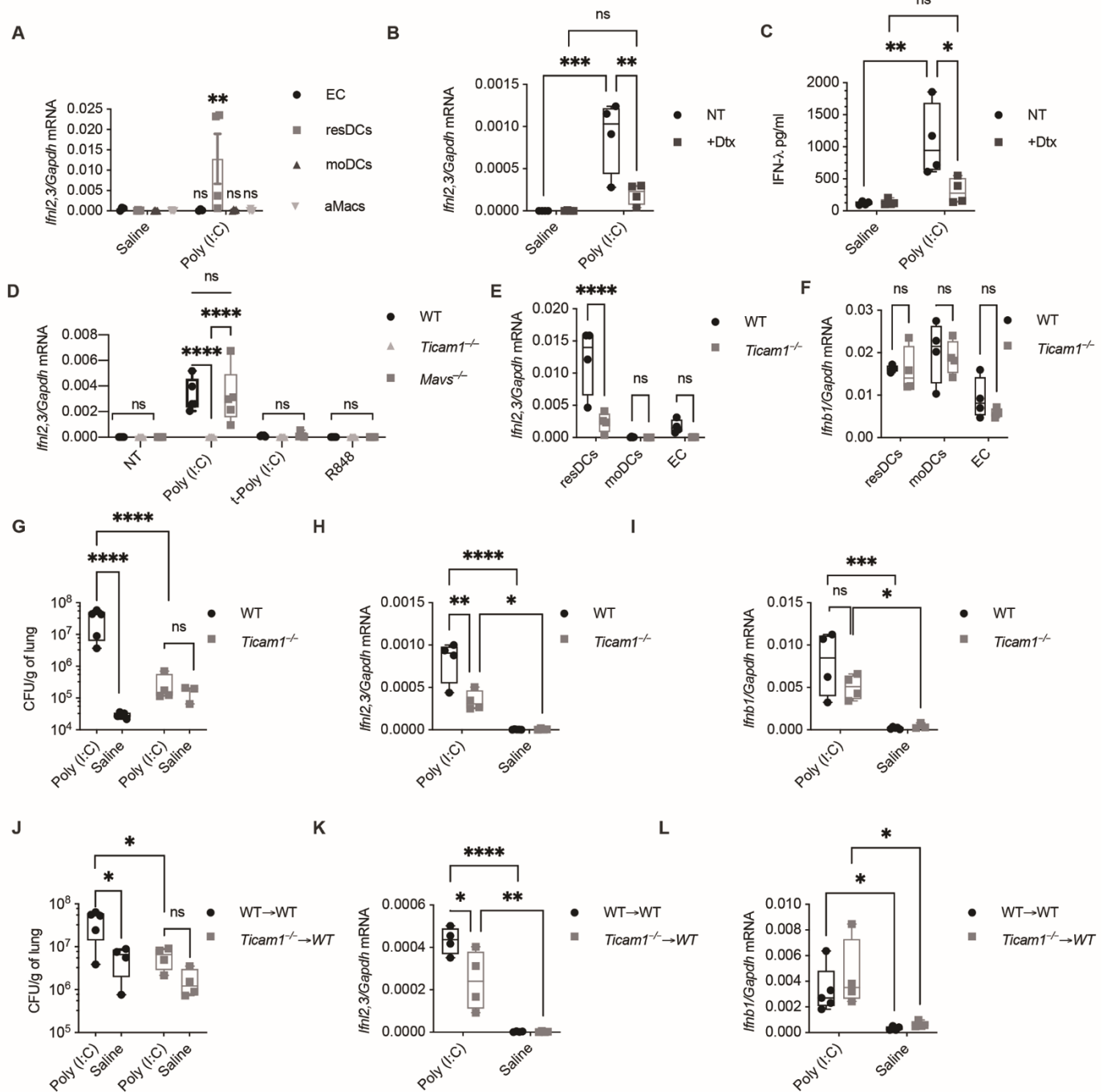


**Fig. 4. Lung resident DCs produce IFN-λ downstream of TLR3 upon viral recognition.** (A) *Ifnl2,3* relative mRNA expression in sorted lung epithelial cells (EC), resident DCs (resDCs), monocytes derived DCs (moDCs), and alveolar macrophages (aMacs) sorted from WT mice i.t. treated with 2.5 mg/kg poly (I:C) or saline daily for 6 days was measured on day 6. (B) CD11c-DTR mice were injected with diphtheria toxin (DTx) to deplete the CD11c<sup>+</sup> cells in vivo. Relative *Ifnl2,3* mRNA (B) and IFN-λ protein levels (C) from lung homogenates were evaluated on day 6. (D) DCs differentiated from bone marrow cells in the presence of FMS-like tyrosine kinase 3 ligand (Flt3l) for 9 days (Flt3l-DCs) from WT, *Ticam1*<sup>-/-</sup>, or *Mavs*<sup>-/-</sup> mice were treated with 50 μg/ml poly (I:C), 1 μg transfected poly (I:C) per 10<sup>6</sup> cells, or 50 μg/ml R848 for 3 hours. Relative *Ifnl2,3* mRNA expression was evaluated by qPCR. *Ifnl2,3* (E), and *Ifnb1* (F) relative mRNA expression in sorted lung epithelial cells (EC), resDCs, and moDCs sorted from WT and *Ticam1*<sup>-/-</sup> mice treated as in (A) was measured on day 6. (G to I) WT and *Ticam1*<sup>-/-</sup> mice were treated with poly (I:C) as in (A) and subsequently i.t. infected with 5 × 10<sup>7</sup> CFU of *S. aureus* on day 6 for 12 hours. Lung bacterial burden normalized by lung weight (G), *Ifnl2,3* (H), and *Ifnb1* (I) relative mRNA expression were evaluated. (J and L) WT chimeric mice reconstituted with *Ticam1*<sup>-/-</sup> bone marrow (*Ticam1*<sup>-/-</sup> → WT) or WT bone marrow (WT → WT) were treated as in (G) to (I). Lung bacterial burden normalized by lung weight (J), *Ifnl2,3* (K) and *Ifnb1* (L) relative mRNA expressions 12 hpi were evaluated. Representative data of three independent experiments. Statistics: ns, not significant ( $P > 0.05$ ); \* $P < 0.05$ , \*\* $P < 0.01$ , \*\*\* $P < 0.001$ , and \*\*\*\* $P < 0.0001$  (Two-way ANOVA). (G to L) (A to C, E to L) Four mice per group, median and range are depicted. (A to F) Mean ± SEM of four mice (A to C, E, F), and of three independent experiments (D) are depicted.

## Type III interferons disrupt the lung epithelial barrier upon viral recognition

Achille Broggi, Sreya Ghosh, Benedetta Sposito, Roberto Spreafico, Fabio Balzarini, Antonino Lo Cascio, Nicola Clementi, Maria De Santis, Nicasio Mancini, Francesca Granucci and Ivan Zanoni

published online June 11, 2020

### ARTICLE TOOLS

<http://science.sciencemag.org/content/early/2020/06/10/science.abc3545>

### SUPPLEMENTARY MATERIALS

<http://science.sciencemag.org/content/suppl/2020/06/10/science.abc3545.DC1>

### REFERENCES

This article cites 30 articles, 10 of which you can access for free  
<http://science.sciencemag.org/content/early/2020/06/10/science.abc3545#BIBL>

### PERMISSIONS

<http://www.sciencemag.org/help/reprints-and-permissions>

Use of this article is subject to the [Terms of Service](#)

---

*Science* (print ISSN 0036-8075; online ISSN 1095-9203) is published by the American Association for the Advancement of Science, 1200 New York Avenue NW, Washington, DC 20005. The title *Science* is a registered trademark of AAAS.

Copyright © 2020 The Authors, some rights reserved; exclusive licensee American Association for the Advancement of Science. No claim to original U.S. Government Works